

Organic–inorganic hybrid proton exchange membranes based on silicon-containing polyacrylate nanoparticles with phosphotungstic acid

Xuejun Cui^a, Shuangling Zhong^b, Hongyan Wang^{a,*}

^a Department of Chemistry, Jilin University, Changchun 130012, PR China

^b Alan G MacDiarmid Institute, Department of Chemistry, Jilin University, Changchun 130012, PR China

Received 25 June 2007; received in revised form 12 August 2007; accepted 13 August 2007

Available online 19 August 2007

Abstract

A series of silicon-containing polyacrylate nanoparticles (SiPANPs) were successfully synthesized by simple emulsifier-free emulsion polymerization technique. The resulting latex particles were characterized by Fourier transform infrared (FTIR) spectrometry, dynamic light scattering (DLS) analysis, thermogravimetric analysis (TGA) and differential scanning calorimetry (DSC). The SiPANP membranes and SiPANP/phosphotungstic acid (SiPANP/PWA) hybrid membranes were also prepared and characterized to evaluate their potential as proton exchange membranes in proton exchange membrane fuel cell (PEMFC). Compared with the pure SiPANP membrane, the hybrid membranes displayed lower thermal stability. However, the degradation temperatures were still above 190 °C, satisfying the requirement of thermal stability for PEMFC operation. In addition, the hybrid membranes showed lower water uptake but higher proton conductivity than the SiPANP precursor. The proton conductivity of the hybrid membranes was in the range of 10^{-3} to 10^{-2} S cm⁻¹ and increased gradually with PWA content and temperature. The excellent hydrolytic stability was also observed in the hybrid membranes because of the existence of crosslinked silica network. The good thermal stability, reasonable water uptake, excellent hydrolytic stability, suitable proton conductivity and cost effectiveness make these hybrids quite attractive as proton exchange membranes for PEMFC applications.

© 2007 Elsevier B.V. All rights reserved.

Keywords: Silicon-containing polyacrylate nanoparticles; Emulsifier-free emulsion polymerization; Phosphotungstic acid; Hybrid membranes; Proton exchange membrane fuel cell

1. Introduction

The proton exchange membrane fuel cell (PEMFC) is considered as one of the most promising power sources due to its wide applications in vehicular transportation and portable electronic devices [1–3]. As a key component of PEMFC, the proton exchange membrane (PEM) should combine following properties: easily synthesized from available and inexpensive raw materials; good film-forming capability; high chemical, mechanical and thermal stabilities; reasonable electrochemical properties [4,5]. To date, perfluorinated polymers such as Nafion[®] have been perceived as the most suitable PEMs

used in PEMFC because of their excellent chemical and physical properties and high proton conductivity. However, the expensive cost, high methanol permeability, loss of conductivity at high temperature (>80 °C) and difficulty in synthesis and processing have limited their wide commercialization [6,7]. To improve the performance of PEM, considerable efforts have been devoted to modify Nafion[®] membrane or to develop alternative new nonperfluorinated PEM materials [8–11].

In recent years, organic–inorganic hybrids have received a great deal of attention due to their advantages in improving mechanical and thermal properties as well as proton conductivity [12–19]. Among them, the hybrids doped with highly conductive heteropolyacids (HPAs) such as phosphotungstic acid (PWA) and silicotungstic acid have exhibited excellent performance and encouraging results [12–16]. However, the heteropolyacids

* Corresponding author. Tel.: +86 431 85168470; fax: +86 431 85175863.
E-mail address: wang_hy@jlu.edu.cn (H. Wang).

may leak out from the PEMs during fuel cell operation due to their water-solubility, which will induce the decline of fuel cell performance. To resolve this problem and to increase the lifetime of fuel cell, heteropolyacids must be fixed in polymer matrix.

In this paper, we synthesized a series of silicon-containing polyacrylate nanoparticles (SiPANPs) via emulsifier-free emulsion polymerization method and prepared the SiPANP/PWA hybrid membranes to obtain satisfactorily proton conductive, chemically and thermally stable PEM materials that are inexpensive and can be simply fabricated. First, compared with the traditional emulsion or miniemulsion polymerization, the emulsifier-free emulsion polymerization provides many advantages: excellent shear stability, monodisperse particle size distribution, and no residuum of emulsifier during membrane formation (avoiding the influence of emulsifier on the membrane performance) [20,21]. Hence, it is a facile and promising method in preparing environment friendly PEM materials. Next, the incorporation of Si(OR)₃ groups during emulsion polymerization using vinyltriethoxysilicone (VTES) as a functional (co)monomer could offer two functions: on the one hand, silicon-containing polymers can present attractive thermal and chemical stability [22]; on the other hand, the hydrolysis and condensation reactions of Si(OR)₃ groups will construct a crosslinked silica network [23–25]. The crosslinked silica network could not only improve the stability, water retention and mechanical strength of membranes but also fix the HPA molecules in the polymer matrix tightly [16,26–28]. Hence, the membranes with silica network may have good potential in fuel cell applications. It is well known that PWA is one of the most attractive inorganic modifiers for proton exchange membranes because of its high proton conductivity and thermal stability [29,30]. When PWA is embedded in SiPANP matrix, the resultant hybrid membranes are expected to possess high proton conductivity in the case of retaining the inherent properties of SiPANP. Accordingly, modification of SiPANP membranes by doping with PWA was tried in this paper and the performances of hybrid membranes were investigated to evaluate their suitability as proton exchange membranes for PEMFC applications.

2. Experimental

2.1. Materials

Styrene (St, 99+%, Aldrich) and butyl acrylate (BA, 99+%, Aldrich) were distilled under a nitrogen atmosphere and reduced pressure prior to polymerization. Methacrylic acid (MAA, 99+%, Aldrich), vinyltriethoxysilicone (VTES, 98+%) and triethylene glycol dimethacrylate (TrEGDMA) were used as received. 4-Styrenesulfonic acid, sodium salt hydrate (NaSS, 99+%), was used without further purification. Ammonium persulfate (APS) and phosphotungstic acid (PWA) were obtained from Aldrich and used as received. The water used in this experiment was distilled followed by deionization.

2.2. Synthesis of the silicon-containing polyacrylate nanoparticles

The silicon-containing polyacrylate nanoparticles (SiPANPs) were prepared by emulsifier-free emulsion polymerization method. The polymerization was carried out under nitrogen atmosphere in a 250 ml four-neck flask equipped with reflux condenser, mechanical stirrer, drop funnel and inlet for nitrogen gas. The flask was first charged with 90 ml of water and 0.1 g of NaSS. After complete dissolution of NaSS in water, the mixture of 2.5 ml of St, 10 ml of BA, 1.0 ml of VTES, 0.5 ml of TrEGDMA and appropriate MAA was added into the flask. Then the flask was placed in water bath and heated to 75 °C with a stirring rate of 300 rpm. After additional 30 min equilibration time, the APS aqueous solution (0.2 g of APS was solved in 10 ml water) was dropped into the above flask in 1 h and the final mixture was reacted at 75 °C until the reaction mixture became white with blue. Then the temperature was raised to 80 °C and kept at this temperature for 1 h. After cooling to room temperature, the obtained latex was purified from the unreacted monomers by repeated dialysis. Reaction schematic for the emulsion polymerization is shown in Scheme 1.

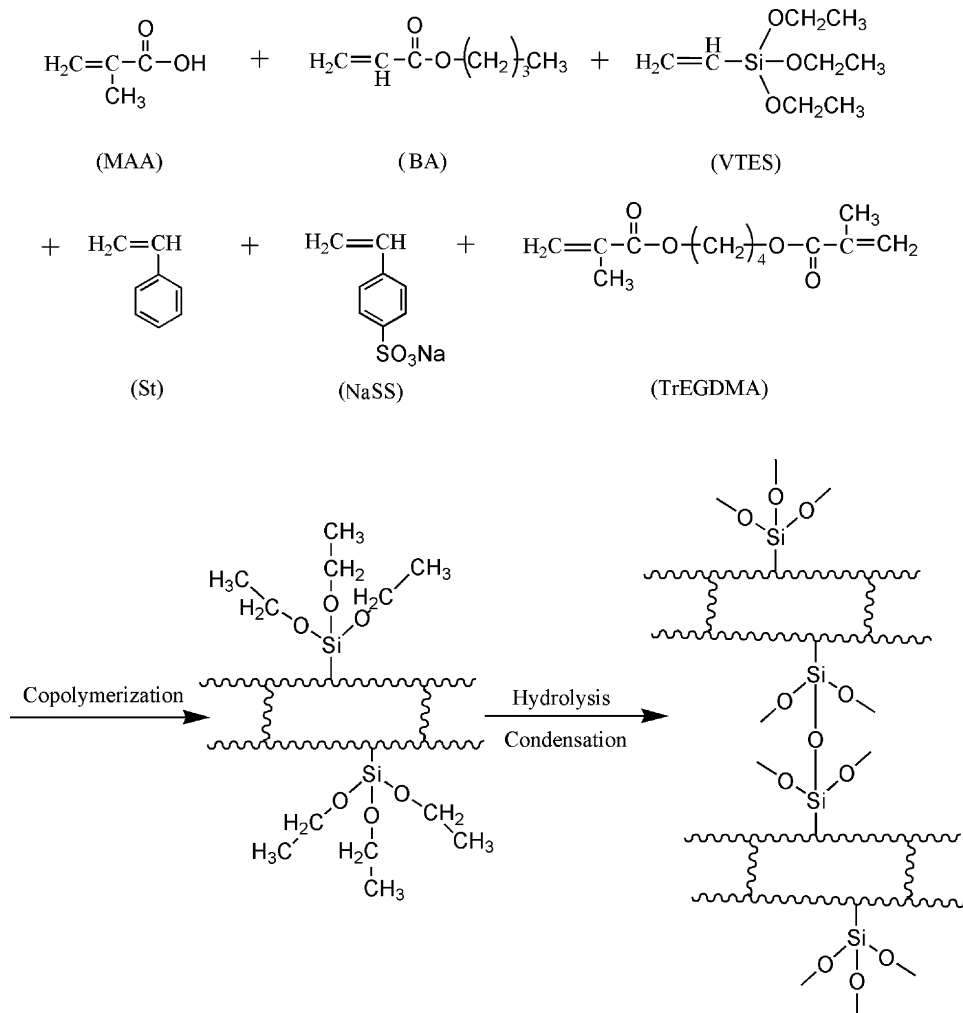
2.3. Membrane preparation

The pure SiPANP membrane was easily obtained by pouring the SiPANP latex into a glass plate and drying at 60 °C for 10 h and 120 °C for 1 h. The amount of carboxylic acid groups in SiPANP1, SiPANP2, SiPANP3 and SiPANP4 membranes were 0.040, 0.074, 0.10 and 0.13 g g⁻¹, respectively. To increase proton conductivity, PWA was introduced into the SiPANP4 precursor. First, the PWA solution with desired concentration was added slowly into SiPANP4 latex and the mixture was stirred for 3 h. Subsequently, the homogeneous solution was cast onto a glass plate and then dried at 60 °C for 10 h and 120 °C for 1 h. The resultant hybrid membrane was rinsed repeatedly with distilled water and stored in distilled water before testing. The hybrid membranes were designated as SiPANP/PWA X, where X is the PWA content (wt.%) in the membrane. The thickness of all membranes was in the range of 90–120 μm.

2.4. Characterization

The FTIR spectra were recorded on a Nicolet Instruments Research Series 5PC Fourier Transform Infrared Spectrometer. For all samples, KBr pellets were prepared and measured in the range from 4000 to 400 cm⁻¹.

The particle sizes and polydispersity of the latex particles were measured by ZetaPALS dynamic light scattering (DLS) detector (BI-90Plus, Brookhaven Instruments Corporation, Holtsville, NY, 15 mW laser, incident beam = 660 nm) at 25 °C. The scattering angle was fixed at 90°. The samples were highly diluted (C < 0.01 wt.%) before testing to prevent multiple scattering. The polydispersity was evaluated through the ratio $\mu_2/(\Gamma)^2$ by cumulants analysis, where μ_2 is the second moment in the cumulants expansion of the correlation function and Γ is the decay rate.



Scheme 1. Reaction schematic for the emulsion polymerization and silica crosslinking.

Thermal stability was detected using a Pyris TGA (Perkin-Elmer). About 3–5 mg sample was preheated to 120 °C and kept at this temperature for 20 min to remove moisture. Then the sample was cooled to 100 °C and reheated to 650 °C at a heating rate of 10 °C min⁻¹ under nitrogen atmosphere.

Differential scanning calorimetry (DSC) measurements were performed on a Mettler Toledo DSC 821e instrument at a heating rate of 10 °C min⁻¹ under N₂ flow.

The water uptake was determined as follows. First, the membrane was vacuum-dried at 100 °C until constant weight was obtained. The dried membrane was then immersed in deionized water for 24 h at different temperatures. Subsequently, the membrane was taken out and immediately weighed after wiping out the surface water. The water uptake was estimated using the expression:

$$\text{water uptake} = \frac{W_{\text{wet}} - W_{\text{dry}}}{W_{\text{dry}}} \times 100\%$$

where W_{wet} and W_{dry} are the weight of the wet and dry membrane, respectively.

The proton conductivity (σ) was measured using an SI 1260+SI 1287 impedance analyzer over the frequency range of 10 to 10⁶ Hz. Before measurement, the membrane was fully hydrated in distilled deionized water for at least 24 h. Then the hydrated membrane was clamped between two stainless steel electrodes and placed in a temperature controlled cell containing distilled deionized water to keep the relative humidity of 100%. The impedance measurement was performed at desired temperature and the proton conductivity was calculated according to the following relationship:

$$\sigma = \frac{d}{Rtw}$$

where d is the distance between the electrodes, t and w the thickness and width of the membranes, respectively, and R is the membrane resistance.

The hydrolytic stability was estimated by soaking the membrane in 80 °C deionized water for 2 weeks and comparing the change of proton conductivity before and after immersion. All the data for each measurement presented in this study are an average of multiple (at least three) experiments and the standard deviations are less than 10%.

3. Results and discussion

3.1. Latex particles analysis

The silicon-containing polyacrylate latexes with high monomer conversion (>95%) have been synthesized successfully and the essential data are listed in Table 1. It is obvious that the particle sizes of the silicon-containing polyacrylate latexes decreased with the increase of MAA content. Generally speaking, the hydrophilic monomer tends to locate on the surface of polymer particles and provides stability to the particles in emulsifier-free emulsion polymerization. Therefore, the colloidal stability increased and particles sizes decreased with increasing amount of hydrophilic monomer MAA [31]. Furthermore, the particle sizes of all the silicon-containing polyacrylate latexes were smaller than that of the polyacrylate latex without silicon. The decrease of particle sizes could be attributed to the incorporation of VTES. The hydrolysis reaction of $\text{Si}(\text{OR})_3$ groups in VTES led to the formation of silanol groups (SiOH). The hydrophilic silanol groups contributed to the increase of colloidal stability and the decrease of particle sizes. In addition, the polydispersity values of all the silicon-containing polyacrylate latex particles were below 0.080, indicating the narrow unimodal distribution of the resultant latex particles.

3.2. FTIR spectra study

The chemical structure of PANP and SiPANP membranes were detected by FTIR and the results are presented in Fig. 1. Compared with the PANP, all SiPANP samples exhibited a new peak at about 1116 cm^{-1} which was attributed to Si-O-Si asymmetric stretching vibration [32]. The appearance of this new peak proved the occurrence of hydrolysis and condensation reactions (crosslinking) of $\text{Si}(\text{OR})_3$ groups and suggested the formation of crosslinked silica network structure in the SiPANP membranes (Scheme 1). The broad peak at around 3260 cm^{-1} was ascribed to $-\text{OH}$ stretching vibration due to the presence of absorbed moisture and COOH groups, and this peak became strong with the increase of MAA content. Furthermore, the COOH peak at 1703 cm^{-1} also showed an increasing tendency as the MAA content increased.

Table 1
Recipes and properties of the silicon-containing polyacrylate latexes

	SiPANP1	SiPANP2	SiPANP3	SiPANP4	PANP
St (ml)	2.5	2.5	2.5	2.5	2.5
BA (ml)	10.0	10.0	10.0	10.0	10.0
MAA (ml)	1.0	2.0	3.0	4.0	4.0
VTES (ml)	1.0	1.0	1.0	1.0	0
TrEGDMA (ml)	0.5	0.5	0.5	0.5	0.5
NaSS (g)	0.1	0.1	0.1	0.1	0.1
APS (g)	0.2	0.2	0.2	0.2	0.2
DI water (g)	100	100	100	100	100
Solid content (%)	11.5	12.3	13.1	13.7	13.8
Conversion (%)	96.7	95.8	96.5	95.6	98.2
Particle size (nm)	167.8	151.9	146.5	131.4	201.0
Polydispersity	0.068	0.020	0.005	0.057	0.110

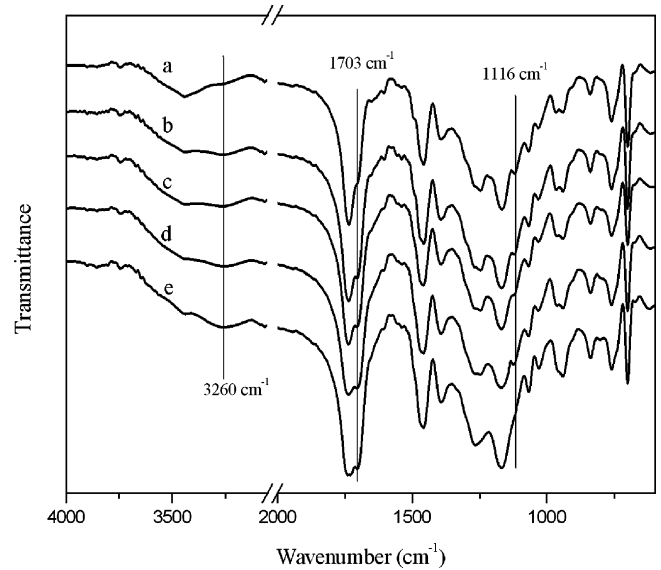


Fig. 1. FTIR spectra of SiPANP1 (a), SiPANP2 (b), SiPANP3 (c), SiPANP4 (d) and PANP (e).

The FTIR spectra of PWA and SiPANP/PWA hybrid membranes were also detected (Fig. 2). The spectrum of pure PWA showed four characteristic bands at 1080 cm^{-1} (P-Oa), 985 cm^{-1} (W=Od), 891 cm^{-1} (W-Ob-W) and 817 cm^{-1} (W-Oc-W) [33]. All these characteristic bands of PWA could be observed in the spectra of hybrid membranes and increased with the increment of PWA content, which indicated that PWA had been incorporated into the SiPANP matrix and confirmed the trend of weight ratio of PWA in hybrid membranes. In addition, the peak at about 1116 cm^{-1} attributed to the Si-O-Si asymmetric stretching vibration could also be observed in the spectra of hybrid membranes, confirming the existence of silica network in hybrid membranes.

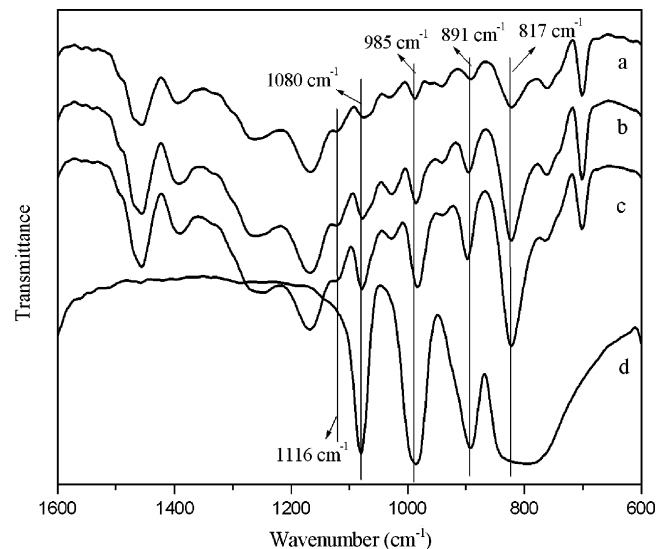


Fig. 2. FTIR spectra of SiPANP/PWA 10 (a), SiPANP/PWA 20 (b), SiPANP/PWA 30 (c) and PWA (d).

3.3. Thermal property

The thermal stability of PANP and SiPANP membranes were measured by TGA. A two-step degradation process could be observed for all the curves in Fig. 3. The first weight loss step from 195 to 300 °C was attributed to the elimination of carboxyl groups, and the mass losses at this temperature range increased with the rise of amount of carboxyl groups. The second thermal degradation began at about 300 °C corresponded to the decomposition of main chain. It can be noted that compared with PANP, the SiPANP4 exhibited higher thermal stability though their carboxyl group contents were same. The improvement in thermal stability was probably due to the introduction of VTES. On the one hand, the hydrolysis and condensation reactions of Si(OR)₃ groups in VTES led to the formation of crosslinked silica network structure. The crosslinked network made the membrane more compact and hence improved the thermal stability [34]. On the other hand, the Si–O bond energy was higher than that of C–C bonds, hence the thermal stability of SiPANP4 was improved due to the formation of Si–O bonds in SiPANP4 with the addition of VTES [35].

Fig. 4 shows the TGA curves of SiPANP4 precursor, PWA and SiPANP/PWA hybrid membranes. It can be seen from Fig. 4 that the thermal stability of SiPANP membrane was decreased in the 190–360 °C range due to the introduction of PWA. The TGA curve of PWA only showed a weight loss at about 150 °C, probably because of dehydration of the water of crystallization, and then no further significant weight loss was observed until 650 °C. Hence while comparing the residual content of hybrid membranes, one can observe that higher residual content was systematically shown by the TGA curves with the increase of PWA content [29]. Although the introduction of PWA decreased the thermal stability of membrane, the degradation temperatures were still above 190 °C. Hence the SiPANP/PWA hybrid membranes were stable enough for use as PEMs in PEMFC.

DSC measurements were carried out to investigate the glass transition temperature (T_g) of PANP and SiPANP/PWA hybrid

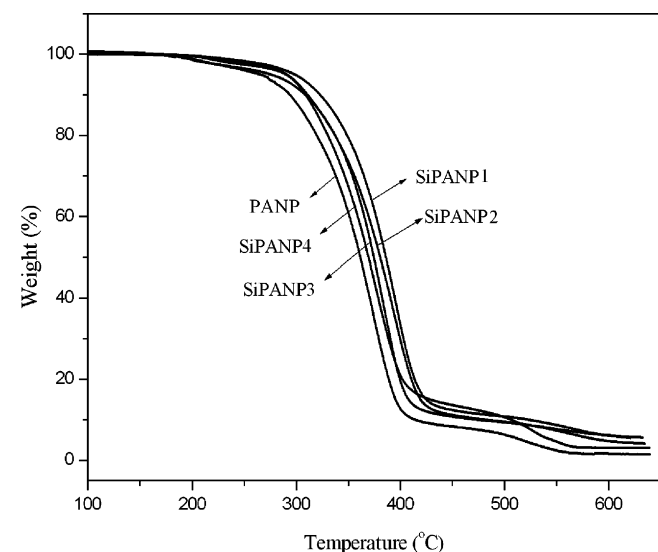


Fig. 3. TGA curves of PANP and SiPANP membranes.

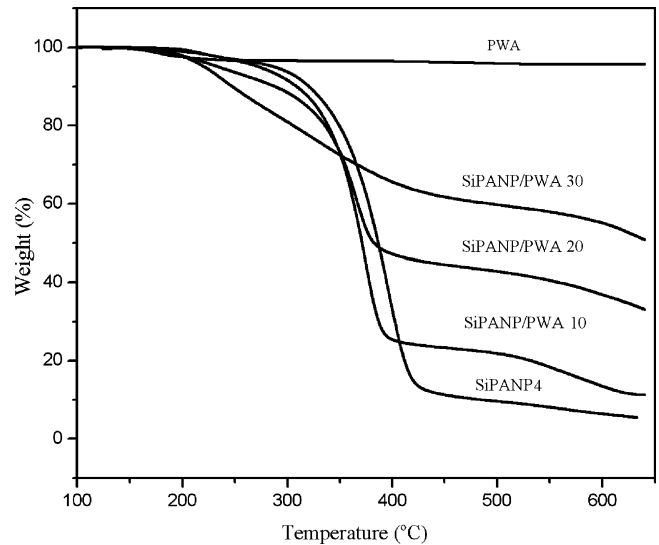


Fig. 4. TGA curves of SiPANP4 and SiPANP/PWA hybrid membranes.

membranes with different PWA contents (Fig. 5). In Fig. 5, only one T_g could be observed for all the samples and SiPANP4 showed higher T_g value than the PANP. The improvement in T_g of SiPANP4 was probably attributed to the reduction in chain mobility due to the formation of crosslinked silica network structure. When PWA was incorporated into the SiPANP matrix, it could be seen that the T_g of hybrid membrane slightly shifted to higher value and improved with increasing amount of PWA. For example, the T_g increased from 42 °C for SiPANP polymer to 52 °C for SiPANP/PWA 30 hybrid membrane. The increment of T_g may be also due to the reduction of chain mobility most probably caused by the intermolecular interaction between carboxylic acid groups in SiPANP polymer chain and PWA fillers [13].

3.4. Water uptake

The water uptakes of PANP and SiPANP membranes with various carboxylic acid contents are shown in Fig. 6 as a function of temperature. For the SiPANP series membranes, the water uptakes increased with increasing carboxylic acid content due to

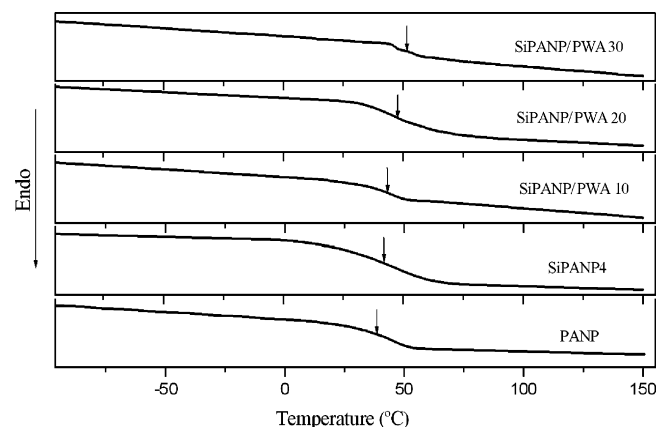


Fig. 5. DSC curves of PANP and SiPANP/PWA hybrid membranes.

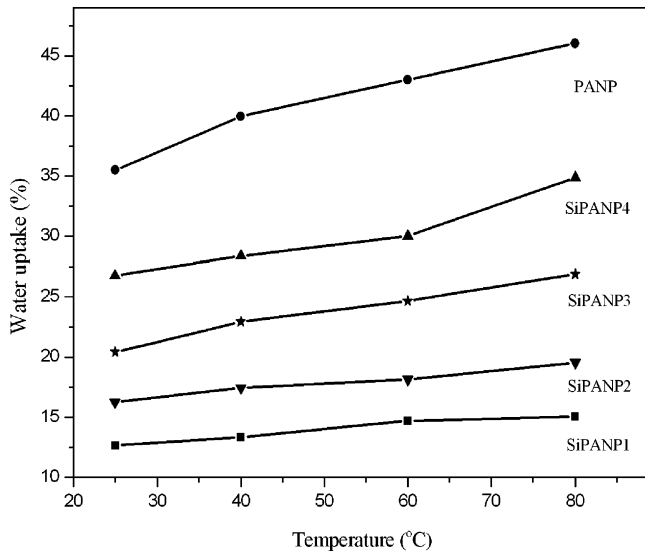


Fig. 6. Water uptake of PANP and SiPANP membranes at different temperatures.

the hydrophilic nature of carboxyl groups. The SiPANP4 membrane possessed the highest water uptake of 26.75% at 25 °C owing to its most carboxylic acid content. However, one can also find from Fig. 6 that the SiPANP4 membrane exhibited much lower water uptake compared with the PANP membrane. Because the amount of carboxylic acid groups was the same in SiPANP4 and PANP, the decrease in water uptake could be attributed to the introduction of crosslinked silica network structure. The crosslinked silica network decreased chain mobility and made the membrane denser and free volume depressed, which effectively repelled water molecules entering the membrane. Consequently, the SiPANP4 membrane with silica network showed lower water uptake compared with the PANP membrane.

After doping with PWA, the water uptakes of SiPANP/PWA hybrid membranes were evaluated and the results are shown in Fig. 7. Interestingly, the water uptakes of hybrid membranes

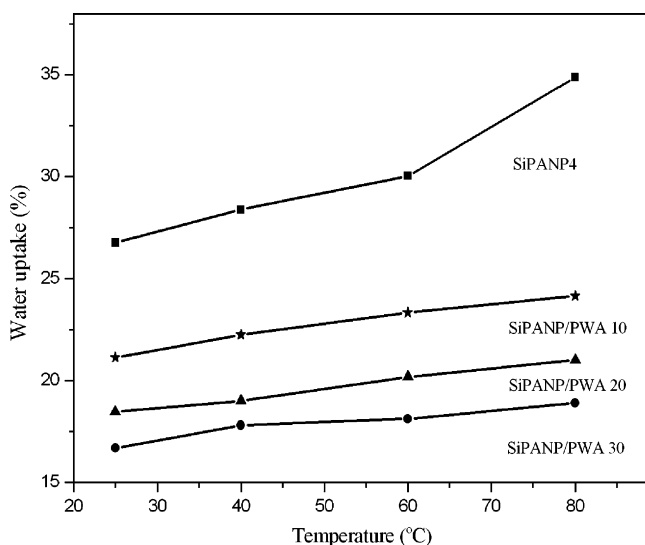


Fig. 7. Water uptake of SiPANP4 and SiPANP/PWA hybrid membranes at different temperatures.

decreased with the increase of PWA content. For example, the water uptake of pure SiPANP4 was 26.75% while the water uptake of SiPANP/PWA 30 membrane was only 16.69% at 25 °C. This trend was consistent with that reported by Xu et al. [36]. A possible reason for this phenomenon was that the big PWA molecules introduced into the hybrid membranes occupied a part of free volume of membranes, hence the hybrid membranes became denser and free volume reduced [36]. In addition, the molecular interaction between SiPANP and PWA prevailed against the increase of hydrophilicity. More interaction led to more rigid and compact structure due to addition of more PWA, which hence also induced the decrease in water uptake [30].

In Figs. 6 and 7, one can also observe that the water uptake of all the membranes increased with the increase of temperature. Take SiPANP4 for example, its water uptake ranged from 26.75 to 34.87% when the temperature increased from 25 to 80 °C. This may be because the mobility of polymer chain and the free volume for water adsorption increased when the temperature elevated, hence water molecules could penetrate the membrane more easily and the water uptake increased.

3.5. Proton conductivity

Proton conductivity is a critical property of fuel cell membranes. The proton conductivities of PANP and SiPANP membranes at different temperatures are plotted in Fig. 8. As shown in Fig. 8, the proton conductivities of the SiPANP series membranes increased slightly from 8.62×10^{-4} to $1.86 \times 10^{-3} \text{ S cm}^{-1}$ at 25 °C with increasing carboxylic acid content. If a comparison was made between the PANP and SiPANP4, one can recognize that the conductivity of SiPANP4 was lower than that of PANP despite the same carboxylic acid content. The decrease in proton conductivity was attributed to the introduction of silica network. Introducing silica network into SiPANP4 impaired the flexibility of polymer backbone and inhibited the mobility of acidic groups to move together to form the

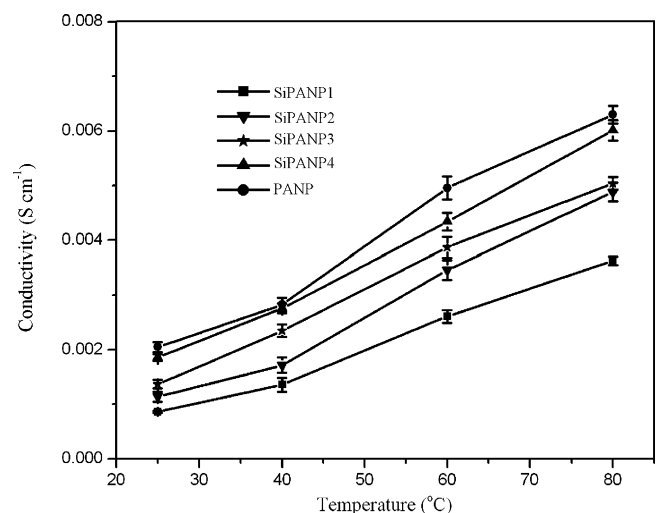


Fig. 8. Proton conductivity of PANP and SiPANP membranes at different temperatures.

ion-rich pathways, which were believed to decrease the proton conductivity of SiPANP4 membrane.

Although the SiPANP materials possessed good stability and moderate water uptake, the low conductivity (10^{-4} to 10^{-3} S cm $^{-1}$) was unsuitable for fuel cell applications. In order to improve the proton conductivity of SiPANP, we prepared and studied the hybrid membranes doped with PWA. The proton conductivities of the SiPANP4 precursor and SiPANP/PWA hybrid membranes with different PWA contents were measured in the temperature range of 25–80 °C and the results are shown in Fig. 9. For comparison, the proton conductivity of Nafion® 117 measured under the same experimental conditions is also plotted in Fig. 9. Though incorporation of PWA decreased the water uptake of SiPANP4 membrane as discussed previously, the conductivity was largely improved and increased with increasing PWA content. When the PWA content achieved 30%, the SiPANP/PWA 30 hybrid membrane showed the highest conductivity values (1.53×10^{-2} S cm $^{-1}$ at 25 °C and 4.10×10^{-2} S cm $^{-1}$ at 80 °C, respectively) which were of the same order of magnitude as the conductivity values of Nafion® 117. The improvement in proton conductivity could be attributed to two reasons: one is the increase of acidity of membrane after PWA incorporation. PWA is a well-known high proton conducting agent. When PWA was introduced into the SiPANP4, it could act as the proton carrier and more PWA provided more protons, hence the proton conductivities of the hybrid membranes were improved [37]. Besides, the proton conductivity was also influenced by the protonic carrier density. Usually, the conductivity should be proportional to the protonic carrier density [38]. The former water uptake results have shown that the increase of PWA content can decrease the water uptake of hybrid membranes, thus the protonic carrier density increased and the energy barrier for the proton transport decreased, which may be also the reason for the observed increase in proton conductivity [39].

It can be seen from Figs. 8 and 9 that every membrane exhibited a positive temperature-conductivity dependency. For

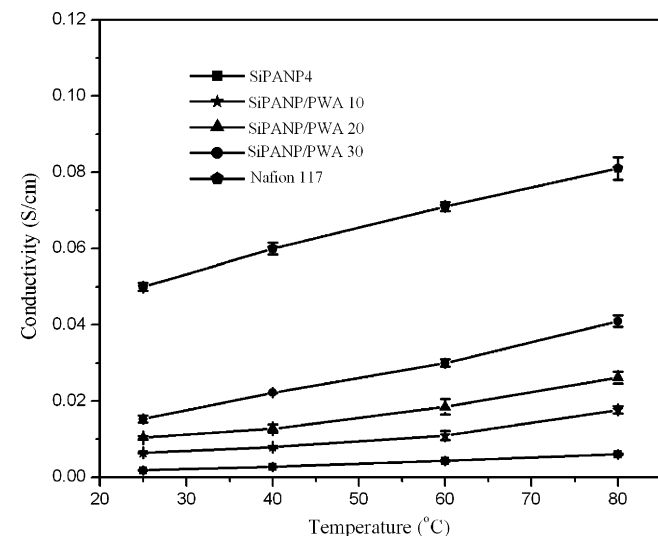


Fig. 9. Proton conductivity of SiPANP4 and SiPANP/PWA hybrid membranes at different temperatures.

example, the proton conductivity of SiPANP/PWA 30 membrane was 1.53×10^{-2} S cm $^{-1}$ at 25 °C and it increased with the temperature to 4.10×10^{-2} S cm $^{-1}$ at 80 °C. It is because that elevating temperature could increase structural reorientation and water uptake as well as mobility of water and proton, and hence favored proton transport [34,40]. When PWA was introduced to the SiPANP4 matrix, the proton conductivities of the most hybrid membranes exceeded 10^{-2} S cm $^{-1}$, indicating the SiPANP/PWA hybrid membranes were suitable as PEMs for fuel cell applications.

3.6. Hydrolytic stability

One of the major problems for the hybrid membranes is the leaking out of dopant from the matrix. Since PWA is water-soluble material, it would be easily removed from the hybrid membranes in the presence of water, which will induce the deterioration of performance of PEM. In order to study the stability of PWA in hybrid membranes, the hydrolytic stability was investigated by comparing the conductivities of hybrid membranes before and after soaking the membranes in 80 °C deionized water for 2 weeks. It is important to mention that the proton conductivities of all hybrid membranes had no visible change after 2 weeks, indicating that the hybrid membranes possessed excellent hydrolytic stability. The good hydrolytic stability suggested that PWA molecules had not or less leaked out from the hybrid membranes during marinating. There might be two factors affecting the hydrolytic stability of membranes. Firstly, the hybrid membranes used in this study had low water uptake, even at high temperature, which could effectively reduce the extraction of PWA. Secondly, after the hydrolysis and condensation reactions of Si(OR) $_3$ groups, the formed silica network could fix PWA molecules tightly and made PWA molecules exist in the hybrid membranes stably [41].

4. Conclusions

A series of silicon-containing polyacrylate nanoparticles (SiPANPs) were successfully synthesized via convenient emulsifier-free emulsion polymerization method. DLS analysis showed that the particle sizes of all the SiPANP latexes were smaller than that of the PANP latex and decreased with the increase of MAA content. Compared with the PANP, the SiPANP membranes exhibited better thermal stability and lower water uptake due to the existence of crosslinked silica network. In addition, the water uptake and proton conductivity of SiPANP membranes increased with the increase of carboxylic acid content, and they varied from 12.67 to 26.75% and from 8.62×10^{-4} to 1.86×10^{-3} S cm $^{-1}$ at 25 °C, respectively.

The SiPANP/PWA hybrid membranes with various PWA contents were also prepared and their suitability as proton exchange membranes for PEMFC applications was investigated. Although the introduction of PWA decreased thermal stability of membrane, the hybrid membranes were still stable enough (thermally stable up to approximately 190 °C) to serve as the PEMs in PEMFC. Furthermore, it is found that the proton conductivity of the hybrid membranes increased with the increasing

PWA content though their water uptake decreased. The maximum proton conductivity ($4.10 \times 10^{-2} \text{ S cm}^{-1}$ at 80°C) could be obtained when the PWA content attained 30%. Moreover, the hybrid membranes exhibited excellent hydrolytic stability and no obvious leak of PWA was observed in the hybrid membranes. These results indicated that the SiPANP/PWA hybrid membranes had good potential in PEMFC applications.

Acknowledgements

This work was supported by the National Natural Science Foundations of China (Grant nos. 50573027 and 50673032).

References

- [1] D.R. Hodgson, B. May, P.L. Adcock, D.P. Davies, *J. Power Sources* 96 (2001) 233–235.
- [2] D.M. Bernardi, M.W. Verbrugge, *J. Electrochem. Soc.* 139 (1992) 2477–2491.
- [3] C. Pan, R.H. He, Q.F. Li, J.O. Jensen, N.J. Bjerrum, H.A. Hjulmand, A.B. Jensen, *J. Power Sources* 145 (2005) 392–398.
- [4] M. Nagai, Y. Chiba, *Solid State Ionics* 176 (2005) 2991–2995.
- [5] J.E. Yang, J.S. Lee, *Electrochim. Acta* 50 (2004) 617–620.
- [6] S. Gamburgzev, A.J. Appleby, *J. Power Sources* 107 (2002) 5–12.
- [7] X.M. Ren, T.E. Spinger, T.A. Zawodzinski, S. Gottesfeld, *J. Electrochem. Soc.* 147 (2000) 466–474.
- [8] K.T. Adjemian, R. Dominey, L. Krishnan, H. Ota, P. Majsztrik, T. Zhang, J. Mann, B. Kirby, L. Gatto, M. Velo-Simpson, J. Leahy, S. Srinivasan, J.B. Benziger, A.B. Bocarsly, *Chem. Mater.* 18 (2006) 2238–2248.
- [9] J.H. Chang, J.H. Park, G.G. Park, C.S. Kim, O.O. Park, *J. Power Sources* 124 (2003) 18–25.
- [10] F. Wang, M. Hickner, Q. Ji, W. Harrison, J. Mechem, T.A. Zawodzinski, J.E. McGrath, *Macromol. Symp.* 175 (2001) 387–395.
- [11] M. Rikukawa, K. Sanui, *Prog. Polym. Sci.* 25 (2000) 1463–1502.
- [12] H.B. Zhang, J.H. Pang, D. Wang, A.Z. Li, X.F. Li, Z.H. Jiang, *J. Membr. Sci.* 264 (2005) 56–64.
- [13] S.M.J. Zaidi, S.D. Mikhailenko, G.P. Robertson, M.D. Guiver, S. Kalanguine, *J. Membr. Sci.* 173 (2000) 17–34.
- [14] P. Staiti, A.S. Aricò, V. Baglio, F. Lufrano, E. Passalacqua, V. Antonucci, *Solid State Ionics* 145 (2001) 101–107.
- [15] C. Yang, P. Costamagna, S. Srinivasan, J. Benziger, A.B. Bocarsly, *J. Power Sources* 103 (2001) 1–9.
- [16] V. Ramani, H.R. Kunz, J.M. Fenton, *J. Membr. Sci.* 279 (2006) 506–512.
- [17] L.C. Klein, Y. Daiko, M. Aparicio, F. Damay, *Polymer* 46 (2005) 4504–4509.
- [18] C.H. Rhee, Y. Kim, J.S. Lee, H.K. Kim, H. Chang, *J. Power Sources* 159 (2006) 1015–1024.
- [19] J. Shen, J.Y. Xi, W.T. Zhu, L.Q. Chen, X.P. Qiu, *J. Power Sources* 159 (2006) 894–899.
- [20] Y. Ohtsuka, H. Kawaguchi, Y. Sugi, *J. Appl. Polym. Sci.* 26 (1981) 1637–1647.
- [21] G.W. Ceska, *J. Appl. Polym. Sci.* 18 (1974) 427–437.
- [22] C.J. Brinker, G.W. Scherer, *Sol–Gel Science: The Physics and Chemistry of Sol–Gel Processing*, Academic Press, Boston, 1990.
- [23] I. Marcu, E.S. Daniels, V.L. Dimonie, C. Hagiopol, J.E. Roberts, M.S. El-Aasser, *Macromolecules* 36 (2003) 328–332.
- [24] T.Y. Guo, C. Xi, G.J. Hao, M.D. Song, B.H. Zhang, *Adv. Polym. Technol.* 24 (2005) 288–295.
- [25] S.Z. Ren, G.Q. Sun, C.N. Li, Z.X. Liang, Z.M. Wu, W. Jin, X. Qin, X.F. Yang, *J. Membr. Sci.* 282 (2006) 450–455.
- [26] I. Honma, H. Nakajima, O. Nishikawa, T. Sugimoto, S. Nomura, *Solid State Ionics* 162/163 (2003) 237–245.
- [27] I. Honma, S. Nomura, H. Nakajima, *J. Membr. Sci.* 185 (2001) 83–94.
- [28] M. Khiterer, D.A. Loy, C.J. Cornelius, C.H. Fujimoto, J.H. Small, T.M. McIntire, K.J. Shea, *Chem. Mater.* 18 (2006) 3665–3673.
- [29] H.W. Zhang, B.K. Zhu, Y.Y. Xu, *Solid State Ionics* 177 (2006) 1123–1128.
- [30] C.W. Lin, R. Thangamuthu, C.J. Yang, *J. Membr. Sci.* 253 (2005) 23–31.
- [31] X.W. Jiang, Y. Wang, W.Q. Zhang, P.W. Zheng, L.Q. Shi, *Macromol. Rapid Commun.* 27 (2006) 1833–1837.
- [32] M. Alagar, S.M. Abdul Majeed, A. Selvaganapathi, P. Gnanasundaram, *Eur. Polym. J.* 42 (2006) 336–347.
- [33] L. Li, Y.X. Wang, *J. Power Sources* 162 (2006) 541–546.
- [34] S. Sundar, W. Jang, C. Lee, Y. Shul, H. Han, *J. Polym. Sci. Part B: Polym. Phys.* 43 (2005) 2370–2379.
- [35] T.Y. Guo, X. Chen, M.D. Song, B.H. Zhang, *J. Appl. Polym. Sci.* 100 (2006) 1824–1830.
- [36] W.L. Xu, C.P. Liu, X.Z. Xue, Y. Su, Y.Z. Lv, W. Xing, T.H. Lu, *Solid State Ionics* 171 (2004) 121–127.
- [37] L. Li, L. Xu, Y.X. Wang, *Mater. Lett.* 57 (2003) 1406–1410.
- [38] W.J. Liang, S.J. Hsieh, C.Y. Hsu, W.F. Chen, P.L. Kuo, *J. Polym. Sci., Part B: Polym. Phys.* 44 (2006) 2135–2144.
- [39] J.L. Qiao, T. Hamaya, T. Okada, *Polymer* 46 (2005) 10809–10816.
- [40] K.D. Kreuer, *Chem. Mater.* 8 (1996) 610–641.
- [41] W.L. Xu, T.H. Lu, C.P. Liu, W. Xing, *Electrochim. Acta* 50 (2005) 3280–3285.